A one-dimensional model for deflagration to detonation transition on the tip of elongated flames in tubes.

Hassan Tofaili, Paul Clavin

Version of Record: https://www.sciencedirect.com/science/article/pii/S0010218021002650
Manuscript_3112d6857cf5458960104faef711ad07

A one-dimensional model for deflagration to detonation transition on the tip of elongated flames in tubes.

Paul Clavin*[a], Hassan Tofaili[b]

[a]*Aix Marseille Université, CNRS, Centrale Marseille, IRPHE UMR7342, 13384 Marseille, France*
[b]*Normandie Université, CNRS, INSA Rouen Normandie, CORIA UMR6614, 76801 Saint-Etienne-du-Rouvray, France*

Abstract

Deflagration-to detonation transition (DDT) of the tip of self-accelerating elongated front of laminar flames in tubes filled with gas mixtures that are very energetic is studied by employing the one-dimensional model sketched in figure 1b. The first part of the present work parallels the nonlinear analysis of the self-similar solution of the double discontinuity model performed by Deshaies and Joulin (1989) (termed DJ herein) in the double limit of weak lead shocks and flame speeds that are very sensitive to the flame temperature. The very energetic mixtures addressed herein exhibit only mild flame-speed dependence on flame temperature but large density ratio so that the critical condition concerns a Mach number of the lead-shock exceeding unity by an amount of order unity. A double-feedback mechanism, in which compressional heating by the lead shock is augmented by an effective piston acceleration due to a back-flow of burnt-gas towards the flame-tip, is shown to yield self-similar solutions that exhibit a turning point at a critical propagation velocity as in DJ but for a lead shock which is not weak. Beyond self-similarity, a further analysis of the upstream-running simple waves generated ahead of the self-accelerating flame then predicts the spontaneous formation of a shock wave on the flame front as a consequence of the finite-time singularity of the acceleration of the flame front at the critical velocity (turning point). Such a shock formation is a good candidate to blow up the inner flame structure, producing the abrupt transition of the flame (a subsonic, quasi-isobaric reaction-diffusion wave) into a detonation (a supersonic compressive wave generating rapid chemical heat release), observed in previously reported experiments, the results of which are consistent with the present scaling.

Keywords: Deflagration-to-detonation transition. Laminar flow. Finite-time singularity.

1. Introduction

Deflagration-to-detonation transition (DDT) remains a poorly understood problem in combustion. Despite more than a century of research, complete identification of the fundamental mechanisms of DDT, namely the abrupt transition from a reaction-diffusion wave (markedly subsonic and quasi-isobaric) to a supersonic reaction wave (a shock generating an exothermic reaction) has not yet been achieved. Ever since the pioneering experiments of Oppenheim and co-workers [1], DDT has been known to develop in various forms and there is no mechanism of DDT that is generally agreed upon as being universal. Reviews are presented in relatively recent textbooks [2, 3] and the state of knowledge in the mid-twentieth century can be found in a Russian book [4]. Considering the double-discontinuity model of a planar shock wave generated by a turbulent flame, treated as a self-propagating discontinuity from the closed end of a tube, Shchelkin and Troshin [4] conjectured that DDT is produced when the flame reaches a velocity large enough to generate a strong shock with a short induction time for igniting the compressed gas. This would require the Mach number of the lead shock $M = \mathcal{D}/a_o$ to be no smaller than $M \approx 5$, necessitating a turbulent flame speed much larger than the laminar flame speed by two orders of magnitude for a typical density ratio. Henceforth, $\mathcal{D}$ denotes the shock velocity and a is the speed of sound, the subscript o identifying conditions in the initial quiescent reactant mixture. Recent experiments [5–8] and numerical simulations by Liberman and coworkers [7, 9] shed new light on DDT of self-accelerating laminar flames propagating in tubes filled with very energetic mixtures (stoichiometric mixtures of hydrogen and oxygen or ethylene and oxygen). The flow ahead of the flame is laminar, and the transition to detonation occurs abruptly, after an exponential acceleration of the tip. The unsteady compression waves that are generated by the accelerating flame, heat the reactive mixture and steepen the shock waves just ahead of the tip of the elongated flame experiencing a sudden transition [6, 7]. The Mach numbers of these shocks are between 2 and 3, and the temperature of the compressed mixture near the axis of the tube does not exceed 850 K, which rules out both the Shchelkin mechanism [4] and the Zel'dovich gradient mechanism [10]. Advanced multi-dimensional numerical simulations have emphasized the role of different mechanisms of

*Corresponding author
Email address: paul.clavin@univ-amu.fr (Hassan Tofaili)

DDT, ranging from the compressible waves in the unreacted mixtures, the viscous dissipation in the boundary layers in micro-channels to the flame instabilities in macro-channels [9, 11, 12]. We will show in the present paper that a simple one-dimensional mechanism, independent of viscous effects, reproduces DDT on the tip of elongated flames in tubes for the same conditions as in the experiments.

More than thirty years ago, Deshaies & Joulin [13] (DJ) published an enlightening theoretical analysis of DDT which was overlooked by the combustion community until 2015-2016, may be due to the fact that the analysis involved a weak lead shock. They derived self-similar solutions of the double-discontinuity model by taking into account the thermal feedback of the lead shock on the flame speed U_T, which for a turbulent flame in the wrinkled-flame-regime is equal to the laminar flame speed U_L multiplied by a constant folding parameter $\sigma > 1$, $U_T = \sigma U_L$. Using the approximation of a small Mach number of the lead shock ($M-1 \ll 1$) and considering high thermal sensitivity $\beta \gg 1$ of the laminar flame speed U_L combined with a large σ in the distinguished limit $\beta\sigma U_L/a_o = O(1)$ where a_o is the sound speed in the initial mixture, DJ showed that the self-similar solutions no longer exist (turning point) above a critical value of σ, roughly $\sigma \gtrsim 10$ for a typical density ratio in ordinary flames. If a sudden transition of a quasi-isobaric flame to a supersonic combustion wave could be systematically produced at the loss of self-similarity (turning point), DDT would have been observed with weakly energetic mixture ($\rho_u/\rho_b \approx 5$) and weak shocks ($M - 1 \ll 1$), contrary to experiments. Additional phenomena should be involved in abrupt DDT. As mentioned by DJ, loss of self-similarity does not mean DDT but only that the unsteady compressible effects cannot be neglected.

Recently, a turning point of the self-similar solutions has also been obtained [14–16] beyond the DJ approximation [13] for different flame models based on the same folding concept.

The unsteady compressible waves upstream a self-accelerating flame have been considered long ago as a key mechanism of DDT [2, 3]. Their dynamics is neglected in the self-similar solutions in which the flow of unreacted gas is uniform between the flame and the lead shock. According to experiments [6, 7], the unsteadiness of the compressible waves plays an important role just before DDT near the axis of the tube; a train of coalescing shock waves is produced in the immediate proximity ahead of the flame. Investigating the coupling with the flame requires the

numerical simulation of the unsteady inner structure of planar flames. This has been performed by Sivashinsky and coworkers [14–16] and in a contribution by Oran and coworkers [17] for flame models that are not realistic. In order to reproduce the critical condition of the self-similar solutions, they addressed fast planar flames having a rate of chemical heat-release (or a rate of molecular diffusion) larger than in gaseous mixtures by two orders of magnitude corresponding to a rate of elastic collisions much larger than in the kinetic theory of gases. Such numerical simulations [14–16] are however instructive; they show a sudden DDT of planar flames as soon as the flame velocity is larger than the critical velocity of the self-similar solutions, typically larger than in real flame by an order of magnitude but still well below the sound speed.

Stimulated by these numerical results [14–16], the first objective of the present paper is to set up a configuration of realistic planar flames showing that the DDT observed in the experiments [6, 7] on the tip of a self-accelerating flame in a tube corresponds to the critical condition of self-similar solutions. The key ingredient of this model, called the piston-model, is the back-flow of burned gas towards the flame tip of an elongated flame. Such a flow has been observed in PIV experiments [18] and also in numerics by Bychkov and coworkers [19, 20] before the formation of the tulip shape. Acting like a piston at the exit of the reaction zone of the planar flame, the back-flow is the mechanism with which the critical condition can be reached by planar laminar flames sustained by a realistic reaction rate. This is all the more true in very energetic mixtures since the density change across the flame is as large as the non-dimensional activation energy (reduced by the enthalpy of the fresh mixture). The corresponding laminar burning velocity is quasi-independent of pressure and increases only mildly with the initial temperature of the mixture. In addition to the successful comparison between the self-similar criticality and the sudden transition observed in the experiments [6, 7], it will be shown that the acceleration of the tip of a self-accelerating flame diverges whatever the growth rate of the elongated front, leading to the formation of a finite-time singularity of the flow on the flame front, followed by the formation of a shock wave. Depending on their intensity, such shocks could blow up the inner structure of the laminar flame quasi-instantaneously, even if the Mach number is not strong enough to produce self-ignition in the unreacted mixture ahead of the flame. The intriguing phenomenon of the abrupt transition observed in experiments cannot be deciphered on the basis of self-similar solutions since

the coupling of the unsteady solution of the inner flame structure with the compression waves is required. A further advantage of the piston-model is that it is ideally suitable to investigate this sharp transient phenomenon inside the inner flame structure for a real (or at least realistic) chemistry of flames, by using the high-order spectral difference flow solver of Lodato [21]. The formulation of the problem is briefly given at the end of the present article, see the legend of figure 3, the numerical analysis being left for future work.

2. Back-flow of burned gas to the tip of an elongated flame. Piston-model

Consider a flame which is ignited punctually at the center of the closed end of a tube. In connection with their revealing experimental investigation of the mechanism by which tulip flames are formed, Clanet and Searby [22] (CS) present a model for the acceleration of the tip of an elongated flame. The flow of burned gas inside the volume delimited by the elongated flame front is fed by the combustion of the lateral wing of the flame skirt, producing a back-flow of burned gas towards the flame tip which is the basic ingredient of the piston model, see figure 1.

2.1. Self-accelerating flame

In a rough approximation, following CS, the flow of burned gas on the axis of the cylindrical tube is modeled by the solution of the one-dimensional equation for the conservation of mass with a source term describing the effect of the combustion of the lateral wings. Neglecting the curvature effect, the tip of the flame front is considered as a planar wave perpendicular to the axis. The flow $u_b(x,t)$ of burned gas is delimited by the wall at $x = 0$ ($u_b = 0$) and the flame at the tip $x = L$ ($u_b = u_{bf}$). Denoting U_L and U_b the laminar flame speeds relative to the fresh mixture and the burned gas respectively, $\rho_u U_L = \rho_b U_b$, ρ_u and ρ_b being the corresponding densities, the rate of mass production per unit volume by the lateral wings of the elongated front is $2\rho_b U_b/R$ where R is the radius of the tube. The laminar flame speed U_L corresponds to the condition of temperature $T = T_u$ and density $\rho = \rho_u$ just ahead of the flame as they are modified by the compression waves propagating in the unreacted mixture just upstream of the flame.

If the rate of increase of the length of the elongated flame $L(t)$ is slow at the scale of the transit time of a fluid particle across the flame, the inner flame structure is quasi-steady. If, in addition,

$\mathrm{d}L/\mathrm{d}t \ll a_b$, $L/(\mathrm{d}L/\mathrm{d}t) \gg L/a_b$, where a_b is the speed of sound in the burned gas, unsteadiness of the compressible effects are negligible in the burned gas, so that the temperature and pressure of the fresh mixture on the lateral wings are the same as at the tip of the elongated flame and the thermodynamic properties of the burnt gas are quasi-uniform and quasi-steady. The variation of density being negligible in the flow of burned gas, the velocity of burned gas $\overline{u}_b(x,t)$ in the laboratory frame increases linearly with the distance from the closed end of the tube ($x = 0$) [22],

$$\mathrm{d}L/\mathrm{d}t \ll a_b \quad \Rightarrow \quad \frac{\partial \overline{u}_b}{\partial x} = 2\frac{\overline{\rho}_{uf}}{\overline{\rho}_{bf}}\frac{U_L}{R} = 2\frac{U_b}{R}, \quad \overline{u}_{bf} = \left(2\frac{L}{R}\right)\frac{\overline{\rho}_{uf}}{\overline{\rho}_{bf}}U_L. \tag{1}$$

Henceforth, the overbar denotes the self-similar solutions and the subscript f refers to the tip of the elongated flame. The inner flame structure being in a quasi-steady state, the flow velocities of burned and unburned gas $\overline{u}_{bf}$ and $\overline{u}_{uf}$ respectively (just behind and ahead the tip of the flame) are related to the velocity of the tip of the flame in the laboratory frame $U_f(t) = \mathrm{d}L/\mathrm{d}t$ by the isobaric conservation of mass $\partial\left(\rho\left[\overline{u} - U_f\right]\right)/\partial x = 0$, $\overline{\rho}_{uf}(U_f - \overline{u}_{uf}) = \overline{\rho}_{bf}(U_f - \overline{u}_{bf})$

$$\frac{L}{\mathrm{d}L/\mathrm{d}t} \gg \tau_L \quad \Rightarrow \quad \overline{u}_{uf} = \frac{\overline{\rho}_{bf}}{\overline{\rho}_{uf}}\overline{u}_{bf} + \left(1 - \frac{\overline{\rho}_{bf}}{\overline{\rho}_{uf}}\right)U_f = 2U_L\frac{L}{R} + \left(1 - \frac{\overline{\rho}_{bf}}{\overline{\rho}_{uf}}\right)U_f. \tag{2}$$

Introducing the laminar flame speed U_L of an unreacted mixture at temperature $\overline{T}_{uf}$

$$U_f = \overline{u}_{uf} + U_L \tag{3}$$

into (2) yields the expressions of $\overline{u}_{uf}$ and U_f in terms of the laminar flame speed $U_L(\overline{T}_u, \overline{\rho}_u)$, the density ratio $\overline{\rho}_{uf}/\overline{\rho}_{bf} = \overline{T}_b/\overline{T}_u > 1$ and the length L of the elongated flame front

$$\overline{u}_{uf} = U_L\frac{\overline{\rho}_{uf}}{\overline{\rho}_{bf}}\sigma - U_L, \quad \frac{U_f}{U_L} = \frac{\overline{\rho}_{uf}}{\overline{\rho}_{bf}}\sigma, \quad \frac{U_f}{U_b} = \sigma, \quad \text{where} \quad \sigma \equiv \left[2\frac{L}{R} + 1\right]. \tag{4}$$

The elongation of the flame (ratio of the flame surface area to the cross-section area of the tube) is characterized by σ. The classical expression of the flow generated ahead of a planar flame when the burned gas is at rest $u_u = (\rho_u/\rho_b - 1)\,U_L$, $U_f = (\rho_u/\rho_b)\,U_L$ is recovered from the first equation (4) for $2L/R = 0$. Equations (2) and (4) are relevant locally at the tip of the elongated flame. The

overall conservation of mass between the closed end of the tube and a cross-section sufficiently ahead of the tip leads to the same flow velocity as in [13] $[(\overline{\rho}_{uf}/\overline{\rho}_{bf}) - 1]\sigma U_L$ where σ denoted the degree of folding of the turbulent wrinkled flame. Here, the local flow velocity $\overline{u}_{uf}$ is much larger, as discussed now. Equations (2-4) correspond to a one-dimensional piston model of a planar flame pushed by a moving piston whose velocity U_P is equal to $\overline{u}_{bf}$,

$$U_P = \overline{u}_{bf} = (\sigma - 1)(\overline{\rho}_{uf}/\overline{\rho}_{bf})U_L, \tag{5}$$

see figure 1-b. The burnt-gas flow $\overline{u}_{bf}$ generated just behind the flame tip by the lateral wing of the elongated flame front, see figure 1-a, is the essential difference from the DJ model of wrinkled flame [13]. Because of a large density ratio $\overline{\rho}_{uf}/\overline{\rho}_{bf} \approx 10$, $U_b/U_L \approx 10$, this flow is large in very energetic mixtures, even when the flame length L is not much larger than the tube diameter. According to (1), the flow of burnt gas $\overline{u}_{bf}$ depends on the laminar flame speed $U_L(\overline{T}_u, \overline{\rho}_u)$ and thus on the shock-induced increase of temperature and density ahead of the flame.

After ignition and before the time at which the skirt of the elongated front leaves the closed end of the tube (namely the time R/U_b for the lateral wing of the flame to reach the lateral wall of the tube), the geometrical relation $U_f(t) = \mathrm{d}L/\mathrm{d}t$, combined with (4) leads to the CS exponential growth of the length of the elongated front [22]

$$\frac{\mathrm{d}(L/R)}{\mathrm{d}t} \equiv \frac{U_f}{R} = \frac{\overline{\rho}_{uf}}{\overline{\rho}_{bf}}\frac{U_L}{R}\left(2\frac{L}{R} + 1\right) = \frac{U_b}{R}\left(2\frac{L}{R} + 1\right) \tag{6}$$

involving the characteristic time scale

$$\tau_{ev} = R/2U_b = (U_{bo}/U_b)\tau_{evo} \quad \text{where} \quad \tau_{evo} = R/2U_{bo} \quad \text{with} \quad U_{bo} = (T_{bo}/T_o)U_{Lo}. \tag{7}$$

According to (6), the conditions for a quasi-steady approximation in the burned gas ($\mathrm{d}L/\mathrm{d}t \ll a_b$) and also inside the flame structure ($d_L/U_b \ll \tau_{evo}$, where d_L is the thickness of the laminar flame) read

$$2\,L/R \ll a_b/U_b = \sqrt{T_u/T_b}\,a_u/U_L \qquad \text{and} \qquad d_L/R \ll 1 \qquad \text{respectively.} \tag{8}$$

However, the acceleration of the tip stops suddenly after a lapse of time of order R/U_L, producing the formation of a tulip flame (associated with the strong deceleration [3, 22]). This phenomenon usually occurs before DDT and is followed by a second stage of weaker acceleration in the DDT experiments [6, 7]. Taking into account the viscous effect, the two-dimensional numerical simulations of flames in a tube with no-slip condition at the wall, carried out by Bychkov and coworkers [19, 20], have shown that a curved flame accelerates during a longer period of time with a growth rate smaller than (7) by a factor depending on the Reynolds number. In the following, the expression (7) of the characteristic time for the growth rate of the length of the elongated flame has to be understood as a dimensional equation, $\tau_{evo} \propto R/2U_{bo}$. The forthcoming results are valid regardless of the numerical coefficient, see the end of § 5. The essential point is that, according to (1)-(5), the flows $u_{bf} = [(\rho_u/\rho_b)(\sigma - 1)U_L$ and $u_{uf} = u_{bf} + (\rho_u/\rho_b - 1)U_L$ are proportional to and much larger than the laminar flame speed $U_L(\overline{T}_u, \overline{\rho}_u)$ in very energetic mixture $\rho_u/\rho_b \approx 10$, $u_{uf} > \overline{u}_{bf} \gg U_L$, even for a moderate elongation $L/R \approx 2$ as in flame bubbles.

2.2. Thermal sensitivity of the flame speed in very energetic mixtures

Because of a large density ratio $\rho_u/\rho_b \approx 10$, the thermal sensitivity of the laminar flame-speed of very energetic mixtures is weaker than for ordinary mixtures. This can be checked on the burning-velocity derived by Zel'dovich and Frank-Kamenetskii [23] for a one-step kinetics scheme governed by an Arrhenius law, in the limit of large Zel'dovich number $\beta_b \equiv [E/(k_B T_b)][q_m/(c_p T_b)] \gg 1$ where q_m and c_p are respectively the heat released and the specific heat capacity per unit mass at constant pressure. The result for a second order reaction is

$$U_L = \frac{\rho_b}{\rho_u}\sqrt{4!\mathrm{Le}^2\frac{1}{\beta_b^3}\frac{D_{Tb}}{\tau_{rb}}} \quad \text{with the reaction rate} \quad \frac{1}{\tau_{rb}} = \left(\frac{\rho_b}{\rho_u}\right) B\,\frac{e^{-E/k_B T_b}}{(\tau_{coll})_b} \tag{9}$$

$$U_L = a_b\left(\frac{\rho_b}{\rho_u}\right)^{3/2} T_b^3 K\, e^{-E/2k_B T_b} = a_b\,(T_b T_u)^{3/2} K\, e^{-E/2k_B T_b}, \quad K \equiv \sqrt{4!B\mathrm{Le}^2\left(\frac{k_B}{E}\frac{c_p}{q_m}\right)^3} \tag{10}$$

where the subscripts u and b denote the unburnt and burnt mixture respectively, Le is the Lewis number, k_B stands for the Boltzmann constant and $1/\tau_{coll}$ represents the (elastic) collision frequency. The derivation of equations (9)-(10) is reproduced in [3]. The relation $D_T/\tau_{coll} = a^2$

has been used in (10) showing that the laminar flame velocity does not depend on the pressure. According to the kinetic theory of gas, the factor B in (9) is of order unity and cannot be large, $B \lesssim 1$. Flames, in general, have contributions from unimolecular, bimolecular, and three-body elementary steps affecting their effective one-step reaction order, but (largely computational) considerations of laminar burning velocities suggest that the bimolecular steps are dominant for highly energetic mixtures, leading to the effective reaction order being close to 2 and thus to a negligible pressure dependence of the constant dimensional factor K (dimension 1/Kelvin$^{3/2}$). The ratio $U_L/a_b \approx (\rho_b/\rho_u)^{3/2}\, e^{-E/2k_BT_b}/\beta_b^{3/2}$ is a small number not larger than $2\,10^{-2}$ in very energetic mixtures ($\rho_b/\rho_u \ll 1$) and much smaller, typically $1.5\,10^{-3}$, in other mixtures ($E/k_BT_b \approx 10$) so that the isobaric approximation $\rho_bT_b = \rho_uT_u$ used in (10) is verified for flames in any premixed gas. Considering the reference state just ahead of the lead shock, denoted by the subscript o, using the relations $a_b/a_{bo} = \sqrt{T_b/T_{bo}}$, $\rho_bT_b = \rho_uT_u$ and $\rho_{bo}T_{bo} = \rho_{uo}T_{uo}$, the laminar flame velocity $U_L(T_u, \rho_u)$ in (10) takes the form

$$\frac{U_L}{U_{Lo}} = \left(\frac{T_b}{T_{bo}}\right)^2 \left(\frac{T_u}{T_{uo}}\right)^{3/2} \exp\left[-\frac{E}{2k_B}\left(\frac{1}{T_b} - \frac{1}{T_{bo}}\right)\right], \tag{11}$$

where $T_b = T_u + q_m/c_p$ and $U_{Lo} \equiv U_L(T_{uo}, \rho_{uo})$ is the laminar flame velocity in the fresh mixture ahead of the shock where temperature and density are T_{uo} and ρ_{uo}, $T_{bo} = T_{uo} + q_m/c_p$. It will be convenient in the self-similar solutions to express the Arrhenius factor in (11) in the form

$$\overline{T}_{bf} - \overline{T}_{uf} = q_m/c_p = T_{bo} - T_o : \quad \mathrm{e}^{-\frac{E}{2k_B}\left(\frac{1}{T_b}-\frac{1}{T_{bo}}\right)} = \mathrm{e}^{\frac{1}{2}\frac{E}{k_BT_{bo}}\frac{(\overline{T}_{bf}-T_{bo})}{\overline{T}_{bf}}} = \mathrm{e}^{\frac{1}{2}\frac{E}{k_BT_{bo}}\frac{(\overline{T}_{uf}-T_o)}{T_o}\left[\frac{T_{bo}}{T_o}+\frac{(\overline{T}_{uf}-T_o)}{T_o}\right]^{-1}}. \tag{12}$$

For very energetic mixtures the temperature ratio $T_b/T_u \approx 10$ is of the same order of magnitude as the activation energy reduced by the initial temperature $E/k_BT_{uo} = 20$, the latter insuring that the initial mixture is frozen far from the chemical equilibrium. Therefore the activation energy, reduced by the enthalpy of the burned gas E/k_BT_b is of order unity, and the exponential factor in (11) does not represent a strong variation of the laminar flame-speed with the flame temperature. The Zeldovich number being of order unity $\beta_b \approx 2$, equations (9)-(11) are questionable. However, they can be employed with a reasonable accuracy, the precise functional dependence of $U_L(T_b)/U_{Lo}$ on

the burnt-gas temperature T_b not being important in our analysis, see the discussion below (27). For example, equation (11) can be replaced by the T_b-dependence of U_L issued from the numerical study of the steady flame-structure. It turns out that (11) provides a good fit with the DDT experiments [6, 7], see § 4.

3. Self-similar solutions.

According to the experimental results [5–8], the abrupt transition to detonation occurs for Mach numbers of the lead shock of order unity $M \in [2.5\,, 3.5]$ that are too small for self ignition of the fresh mixture. For the purpose of comparison with the experimental data, we determine the turning of the self-similar solutions obtained in this section with the one-dimensional piston-model of figure 1.

3.1. Quasi-steady approximation and nonlinear equation

Consider the self-similar solution of the double discontinuity model when the acceleration of the tip of the elongated flame is neglected, $U_f \approx \text{cst}$, $\overline{u}_{uf} \approx \text{cst}$. More precisely, according to (8), the change of the flame velocity is assumed to be sufficiently slow for making the unsteady compressible effects negligible ahead of the flame front. Thus, the flow of fresh mixture is considered as quasi-uniform and quasi-steady in the region delimited by the planar flame and the lead-shock propagating upstream with a constant supersonic velocity $\mathcal{D}$, $M \equiv \mathcal{D}/a_o > 1$, the subscript o denoting the initial gas ahead of the shock wave. In other words the interaction between the flame and the lead shock is considered as instantaneous in the self-similar solutions. This cannot be the case in the vicinity of the turning point where the flame acceleration involves timescales shorter than the transit time of the acoustic waves between the two fronts, especially when the lead shock is far away from the flame, see §§ 5 and 6.

In the self-similar solutions, the quasi-instantaneous feedback of the lead shock on the flame is given by the Rankine-Hugoniot relations at the Neumann state (denoted by the subscript N), expressing the density and temperature of the fresh mixture ahead the flame $\overline{\rho}_{uf} = \rho_N$, $\overline{T}_{uf} = T_N$

in terms of the Mach number M of the shock,

$$\frac{\rho_o}{\rho_N} = \frac{(\gamma-1)M^2+2}{(\gamma+1)M^2}, \quad \frac{u_N}{a_o} = \frac{2}{\gamma+1}\left[M-\frac{1}{M}\right], \quad \frac{T_N}{T_o} = \frac{2\gamma}{(\gamma+1)^2}\left[1-\frac{(\gamma-1)}{2\gamma M^2}\right]\left[2+(\gamma-1)M^2\right], \quad (13)$$

so that the laminar flame speed $U_L(\overline{\rho}_{uf}, \overline{T}_{uf})$ in (11) can be expressed in terms of M. Equation (4) in which the quasi-isobaric approximation of the flame structure $\overline{\rho}_{uf}/\overline{\rho}_{bf} = (\overline{T}_{uf} + q_m/c_p)/\overline{T}_{uf}$ is used, leads to express the flow velocity $\overline{u}_{uf}$ in terms of M and the flame elongation L/R. For a given elongation of the finger flame, the second relation in (13) with $u_N = \overline{u}_{uf}$ then leads to a nonlinear equation for M characterized by a turning point.

3.2. Self-similar solution of the piston-model using the DJ approximation

It is useful to begin the analysis of the self-similar solutions of the piston-model by using the same approximations as in DJ for the turbulent wrinkled flame [13]. Even though these basic approximations are not valid at the critical condition of the finger flames in tubes filled with an energetic mixture, this simplified analysis provides instructive physical insights. A key point of the preceding discussion below (13) is the increase of the Neumann temperature T_N with the flow velocity u_N. For a weak shock $M-1 \ll 1$, neglecting the terms of order $(M-1)^2$ in (13), the temperature jump $T_N/T_o - 1$ increases linearly with u_N/a_o so that the temperature $\overline{T}_{uf}$ and the flow velocity $\overline{u}_{uf}$ of the unreacted gaseous mixture ahead of the flame are linearly related

$$0 < M-1 \ll 1: \qquad \frac{\overline{p}_{uf}}{p_o} - 1 \approx \gamma\frac{\overline{u}_{uf}}{a_o} = \frac{4\gamma}{\gamma+1}(M-1) + .., \qquad \frac{\overline{T}_{uf}}{T_o} - 1 = (\gamma-1)\frac{\overline{u}_{uf}}{a_o} + ..., \quad (14)$$

the only non-linearity left being the high sensitivity of the flame speed to the flame temperature. This is the basic assumption of the DJ analysis leading to an analytical expression of the nonlinear equation for the flame speed. For a large activation energy, the Arrhenius factor (12) reads

$$E/k_BT_{bo} \gg 1, \quad (E/k_BT_{bo})(\overline{T}_{uf}-T_o)/T_{bo} = O(1) \quad \Rightarrow \quad \mathrm{e}^{-\frac{E}{k_B}\left(\frac{1}{\overline{T}_b}-\frac{1}{T_{bo}}\right)} \approx \mathrm{e}^{\frac{1}{2}\frac{E}{k_BT_{bo}}\frac{T_o}{T_{bo}}\frac{(\overline{T}_{uf}-T_o)}{T_o}}. \quad (15)$$

On the one hand, introducing the last equation (14) into (15), equation (11) then gives an expression of the laminar flame speed in terms of the flow velocity $\overline{u}_{uf}$

$$0 < M - 1 \ll 1 \quad : \qquad U_L/U_{Lo} = \mathrm{e}^{\frac{1}{2}\frac{E}{k_B T_{bo}}\frac{T_o}{T_{bo}}(\gamma-1)\frac{\overline{u}_{uf}}{a_o}}. \tag{16}$$

On the other hand, in the piston model, the flow velocity $\overline{u}_{uf}$ is expressed in terms of U_L and L by the first equation (4) into which the density ratio is approximated by $\overline{\rho}_{uf}/\overline{\rho}_{bf} \approx T_{bo}/T_o$ in agreement with the approximation $M - 1 < 1$

$$\overline{u}_{uf}/U_L \approx (T_{bo}/T_o)\big[\, 2L/R + (T_{bo} - T_o)/T_{bo}\big]. \tag{17}$$

Introducing (17) into (16) yields a nonlinear equation for the ratio U_L/U_{Lo}

$$0 < M - 1 \ll 1 : \qquad U_L/U_{Lo} = \mathrm{e}^{\frac{1}{2}\frac{E}{k_B T_{bo}}(\gamma-1)\frac{U_{Lo}}{a_o}\left[(2L/R+1)-\frac{T_o}{T_{bo}}\right]\frac{U_L}{U_{Lo}}}, \tag{18}$$

which is meaningful in the distinguished limit used by DJ, $E/k_B T_{bo} \gg 1$, $\sigma \gg 1$ such that $(\gamma - 1)\sigma(E/k_B T_{bo})(U_{Lo}/a_o) = O(1)$. Using the notation $m \equiv U_L/U_{Lo}$, equation (18) can be written in a form similar to (19) and (20) in [13]

$$m = \mathrm{e}^{S\,m} \quad \text{where} \quad S \equiv b\left[2\frac{L}{R} + \frac{T_{bo} - T_o}{T_{bo}}\right] \quad \text{and} \quad b \equiv \frac{(\gamma-1)}{2}\frac{E}{k_B T_{bo}}\frac{U_{Lo}}{a_o} \ll 1, \tag{19}$$

the relation $b \ll 1$ coming from the fact that the laminar flame speed is substantially subsonic $U_{Lo}/a_o \ll 1$, see (9). In the limit used by DJ for the turbulent flame problem $\sigma \gg 1$: $b\sigma = O(1)$, $S = O(1)$, a turning point is exhibited in (19) by the piston-model for a critical ratio L/R; there is no solution for an elongation S above a critical value $S^* = 1/\mathrm{e}$, $m^* = \mathrm{e}$, while two solutions exist below for $m < m^*$, $S < S^* = 1/\mathrm{e}$, the physical solution being the one for which the unperturbed velocity U_{Lo} is recovered when the thermal effect (14) vanishes $\overline{T}_{uf} \to T_o$, $\overline{u}_{uf} \to 0$, $\lim_{S\to 0} U_L/U_{Lo} = 1$. According to (19), the laminar flame velocity U_L of the physical solutions $m \leqslant m^*$ is still markedly subsonic, $U_L^* = \mathrm{e}\, U_{Lo}$ and the critical length of the elongated flame L^* is substantially larger than the radius of the tube $L^*/R \approx 1/(2\mathrm{e}\, b)$.

A main difference with the forthcoming analysis of the very energetic mixtures in § 3.3 is that the linear relations (14) are no longer accurate. However, two important conclusions can be drawn from this simple calculation. Firstly, the back flow of the elongated flame is essential to reach a critical condition at the tip; this follows from (19) showing that the critical condition can never be attained by a planar flame propagating from the closed end of a tube when the burnt gas is at rest $\overline{u}_{bf} = 0$, the scalar S being well below the critical value 1/e for $L = 0$, $S = b\,(T_{bo} - T_o)/T_{bo}$, still too small by a factor 10^{-1} for $U_{Lo}/a_o \approx 1.6\,10^{-2}$, $T_{bo}/T_o = 10$, $E/k_B T_b \approx 10$, $\gamma = 1.4 \Rightarrow b \approx 0.032$. Moreover, for such a energetic mixture, according to (19), the critical elongation of the flame front is not very large, $2L^*/R + (T_{bo} - T_o)/T_{bo} = 1/(b\mathrm{e}) \approx 10.5$, $L^*/R \approx 5$. Secondly, the critical flow $\overline{u}^*_{fu} \approx 1.76\,a_o$ is supersonic yielding a Mach number of the lead shock close to 2, in contradiction with the the weak shock assumption $M - 1 \ll 1$ in (14). Therefore, one has to be back to the full Rankine-Hugoniot conditions (13).

3.3. Critical condition for elongated flames in tube filled with a very energetic mixture

In this section the self-similar solutions are computed by the method discussed at the end of § 3.1. Assuming that the heat release and the specific heat per unit mass are constant, $\overline{T}_{bf} - \overline{T}_{uf} = T_{bo} - T_o = q_m/c_p$, the density and temperature ratios $\overline{\rho}_{uf}/\overline{\rho}_{bf}$ and $\overline{T}_{bf}/T_{bo}$ to be introduced into (4) and (11), respectively, are expressed in terms of $\overline{T}_{uf}/T_o$

$$\frac{\overline{\rho}_{uf}}{\overline{\rho}_{bf}} = \frac{\overline{T}_{bf}}{\overline{T}_{uf}} = 1 + \frac{\overline{T}_{bf} - \overline{T}_{uf}}{\overline{T}_{uf}} = 1 + \frac{(T_{bo} - T_o)}{\overline{T}_{uf}} = 1 + \frac{q_m/c_p T_o}{\overline{T}_{uf}/T_o}, \tag{20}$$

$$\frac{\overline{T}_{bf}}{T_{bo}} = \frac{\overline{T}_{uf} + q_m/c_p}{T_o + q_m/c_p} = \frac{\overline{T}_{uf}/T_o + q_m/(c_p T_o)}{1 + q_m/(c_p T_o)}, \tag{21}$$

which can be written by using the short notation $y \equiv \overline{T}_{uf}/T_o > 0$ and $q \equiv q_m/c_p T_o > 1$ as

$$\frac{\overline{\rho}_{uf}}{\overline{\rho}_{bf}} = 1 + \frac{q}{y}, \qquad \frac{\overline{T}_{bf}}{T_{bo}} = \frac{y+q}{1+q}, \quad \text{where} \quad y \equiv \frac{\overline{T}_{uf}}{T_o} \quad \text{and} \quad q \equiv \frac{q_m}{c_p T_o} = \frac{T_{bo} - T_o}{T_o}. \tag{22}$$

According to the Rankine-Hugoniot equation (13) for T_N/T_o with $T_N = \overline{T}_{uf}$, the scalar y in (22) is a function of M^2. The algebra in (13) simplifies by anticipating that $\gamma - 1 \approx 0.3 - 0.4$ is negligible

in front of $2\gamma M^2$ near criticality, which is the case as soon as $M^* \gtrsim 2$,

$$\frac{2\gamma M^2}{\gamma-1} \gg 1 : \qquad \frac{\overline{T}_{uf}}{T_o} \approx \frac{2\gamma}{(\gamma+1)^2}[2+(\gamma-1)M^2], \quad y\,(M^2) = \frac{2\gamma}{(\gamma+1)^2}[2+(\gamma-1)M^2] \tag{23}$$

The flow velocity $\overline{u}_{uf}$, generated ahead of the flame in (4),

$$\frac{\overline{u}_{uf}}{a_o} \approx \frac{U_L}{U_{Lo}}\frac{U_{Lo}}{a_o}\left[\left(1+\frac{q}{y}\right)\sigma - 1\right] \quad \text{where} \quad \sigma \equiv \frac{2L}{R}+1 \tag{24}$$

then takes the form of a function of M^2 when the ratio U_L/U_{Lo} is expressed in terms of $y\,(M^2)$ by using (11) in which, according to (22), $1/\overline{T}_{bf} - 1/T_o = (1/T_o)(1-y)/(y+q)$

$$\frac{\overline{u}_{uf}}{a_o} = \frac{U_{Lo}}{a_o}\left[\left(1+\frac{q}{y}\right)\sigma - 1\right]\left(\frac{y+q}{1+q}\right)^2 y^{3/2}\exp\left[\frac{\beta_o(y-1)}{(y+q)}\right] \quad \text{where} \quad \beta_o \equiv \frac{E}{2k_B T_{bo}} = O(1). \tag{25}$$

For a given reactive mixture characterized by the set of parameters (U_{Lo}/a_o, q, β_o and γ), the first Rankine-Hugoniot relation (13) $u_N/a_o = \overline{u}_{uf}/a_o = 2(M-1/M)/(\gamma+1)$, combined with (25), leads to a nonlinear equation for M parametrized by the parameter σ characterizing the elongation L/R. This equation takes a simpler form if $(1+q/y)\,\sigma \gg 1$ which is the case for a large heat release $q \approx 10$ (very energetic mixtures) so that the elongation of the flame $\sigma = 2L/R+1$ appears as a factor in the right-hand side of (25). The equation for M then takes the form

$$\Lambda^{-1}\mathcal{L}(M) = \mathcal{R}(M), \quad \text{where} \quad \mathcal{L}(M) \equiv \frac{M-1/M}{1+q/y}, \qquad \Lambda \equiv \frac{\gamma+1}{2}\frac{U_{Lo}}{a_o}\,\sigma \tag{26}$$

$$\text{and} \qquad \mathcal{R}(M) \equiv \frac{U_L}{U_{Lo}} = \left(\frac{y+q}{1+q}\right)^2 y^{3/2}\exp\left[\frac{\beta_o(y-1)}{(y+q)}\right] \tag{27}$$

where the elongation σ appears only in the coefficient Λ and the laminar flame-speed U_L only in $\mathcal{R}(M)$. According to (23), $\mathcal{L}(M)$ and $\mathcal{R}(M)$ are increasing functions of M in the range $M > 1$, involving two parameters (in addition to the ratio of specific heats γ), the reduced heat release $q \approx 10$ and the reduced activation energy $\beta_o \approx 2$ for very energetic mixtures. However the function $\mathcal{R}(M)$ increases more rapidly than $\mathcal{L}(M)$ when M increases while the function $\mathcal{L}(M)$ goes to zero and $\mathcal{R}(M)$ approaches unity in the limit $M-1 \to 0^+$. This is true for the laminar flame-speed of

any energetic mixture, so that the method is not limited to the particular expression (11) of U_L/U_{Lo} used in (27).

The roots of (26) correspond to the intersection of the two graphs $\Lambda^{-1}\mathcal{L}(M)$ and $\mathcal{R}(M)$. When the parameter Λ is too large, namely for either a large elongation σ or a large flame-speed U_{Lo}/a_o, the function $\Lambda^{-1}\mathcal{L}(M)$ is smaller than $\mathcal{R}(M)$ everywhere $\forall\ M \geqslant 1$ so that equation (26) has no roots and there is no self-similar solution of the complex flame-shock, see figure 2. Decreasing Λ, a critical value Λ^* is obtained when the two graphs become tangent at a critical value M^* corresponding to a turning point of the self-similar solutions like in § 3.2, see figure 2. For a small elongation $\Lambda < \Lambda^*$ there are two solutions and the physical one belongs to the branch for which the elongation L/R decreases with $M-1$, since it is a stable branch according to (28). The critical elongation corresponding to Λ^* is easily obtained as follows. For typical values of the parameters $(q,\ \beta_o,\ \gamma)$, the ratio $\mathcal{R}(M)/\mathcal{L}(M)$ first decreases and then increases when M increases from $M=1$ so that it goes through a minimum. This is because the function $\mathcal{R}(M)$ increases more strongly than $\mathcal{L}(M)$ for large M, but $\mathcal{L}(M)$ goes to zero in the opposite limit $M-1 \to 0^+$ while $\mathcal{R}(M)$ goes to a number close to unity. The minimum of $\mathcal{R}(M)/\mathcal{L}(M)$ corresponds to the critical Mach number $M=M^*$ yielding the critical elongation Λ^* given by the ratio $\mathcal{R}(M^*)/\mathcal{L}(M^*) = 1/\Lambda^*$.

4. Comparison with the experimental data.

The critical condition obtained from (26)-(27) is now compared with the experiments [6, 7] in which DDT is observed for $M \in [2.5,\ 3]$. Using a set of parameters corresponding to very energetic mixtures similar to those used in these experiments, $U_{Lo} = 8.54\,\mathrm{m/s}$ ($U_{Lo}/a_o = 0.016$), $T_b/T_o = 10$ ($q=9$), $E/k_BT_o = 25$ ($\beta_o = 1.25$), $\nu = 2$ and $\gamma = 1.4$, the critical condition for the loss of self-similarity obtained from (26)-(27) is $M^* = 2.5$ and $\Lambda^* = 0.089$ (see figure 2), that is $\sigma^* = 4.63$. The corresponding critical values of the temperature ratio $\overline{T}_{uf}/T_o$ and the flame velocity in the laboratory frame U_f are $\overline{T}^*_{uf}/T_o = 2.19$ and $U_f^* \approx 890\,\mathrm{m/s}$ respectively. These values are in good agreement with M and U_f measured just before the abrupt transition in the experiments [6, 7], occurring near the tube axis on the tip of the curved flame front at the end of a second stage of flame acceleration (sometimes after the transient formation of a tulip shape). Moreover $\sigma^* = 4.63$ leads to a small elongation $L^*/R \approx 2$ which is in relatively good agreement with the

curved flame front at the transition visualized by shadow photographs. Interesting enough is the large flow velocity of gas ahead of the flame $\overline{u}^*_{uf} \approx 928\,\mathrm{m/s}$ which is supersonic $\overline{u}^*_{uf}/\overline{a}^*_{uf}$=1.18 ($\overline{a}^*_{uf}/a_o = 1.48$) but subsonic relatively to the lead shock at it should be $(\mathcal{D}^* - \overline{u}^*_{uf})/\overline{a}^*_{uf} \approx 0.5$. Moreover the laminar flame velocity at the transition $U^*_L/U_{Lo} = 4.62$ is still markedly subsonic $U^*_L \approx 39\mathrm{m/s}$, $U^*_L/\overline{a}^*_{uf} \approx 0.05$. The large ratio $\overline{u}^*_{uf}/U^*_L \approx 25$ is due to the large density ratio across the laminar flame $\overline{\rho}_u/\overline{\rho}_b \approx 10$. These results are in good agreement with the experimental data.

To conclude this section, the sudden DDT of self-accelerating elongated flames propagating in tubes filled with very energetic mixtures seems to occur nearby the critical condition of the turning point of the self-similar solutions obtained with the planar piston-model.

5. Finite-time singularity of the acceleration of the flame

A runaway of the acceleration of the flame front (not of its speed) in the self-similar solutions occurs systematically at the turning point when the elongation increases with the time $\sigma(t)$. Introducing the notations $\mathcal{L}'(M)$ and $\mathcal{R}'(M)$ for $\mathrm{d}\mathcal{L}(M)/\mathrm{d}M$ and $\mathrm{d}\mathcal{R}(M)/\mathrm{d}M$ respectively, the time derivative of equation (26) where $\Lambda(t)$ is proportional to $\sigma(t)$,

$$\left[\Lambda^{-1}\mathcal{L}'(M) - \mathcal{R}'(M)\right]\frac{\mathrm{d}M}{\mathrm{d}t} = \mathcal{R}(M)\frac{1}{\Lambda}\frac{\mathrm{d}\Lambda}{\mathrm{d}t} \tag{28}$$

shows that the derivative $\mathrm{d}M/\mathrm{d}t$ increases when the critical value M^* is approached from below and diverges at $M = M^*$, $\lim_{M\to M^*} \mathrm{d}M/\mathrm{d}t = \infty$. The tangency of the two graphs at the critical root M^* of $\mathcal{L}(M) = \Lambda(t)\,\mathcal{R}(M)$ corresponds to $\mathcal{L}'(M^*) = \Lambda^*\,\mathcal{R}'(M^*)$ so that the factor of $\mathrm{d}M/\mathrm{d}t$ on the left-hand side of (28) vanishes while the left-hand side is finite. Expanding the factor on the left-hand side in powers of $M - M^*$, equation (28) takes the form

$$\frac{(M - M^*)}{M^{*2}}\frac{\mathrm{d}M}{\mathrm{d}t} \propto \frac{1}{\Lambda^*}\left(\frac{\mathrm{d}\Lambda}{\mathrm{d}t}\right)_{\Lambda=\Lambda^*} \tag{29}$$

where the constant of proportionality is linearly related to the inverse of the difference of curvature of the graphs at $M = M^*$ in figure 2. The flame velocity in the laboratory frame $U_f(t)$ satisfies a

similar equation near the critical condition

$$U_f \leqslant U_f^*, \qquad \frac{(U_f - U_f^*)}{U_f^*}\frac{1}{U_f^*}\frac{\mathrm{d}U_f}{\mathrm{d}t} \propto \frac{1}{\sigma^*}\frac{\mathrm{d}\sigma}{\mathrm{d}t}\Big|_{\sigma=\sigma^*} \tag{30}$$

where, the definition of Λ in (26) has been used. The elongation growth rate appears here for the first time in the analysis. Introducing the time t^* at which the critical speed is reached $M(t^*) = M^*$, $U_f(t^*) = U_f^*$, $\overline{u}_{uf}(t^*) = \overline{u}_{uf}^*$, and a reference time t_e^* proportional to the inverse of the elongation rate, $1/t_e^* \propto \sigma^{-1}(\mathrm{d}\sigma/\mathrm{d}t)|_{\sigma=\sigma^*}$ integrating (30) yields

$$t - t^* \to 0^- : \qquad \frac{(U_f^* - U_f)}{U_f^*} = \sqrt{\frac{t^* - t}{t_e^*}}, \qquad \frac{t_e^*}{U_f^*}\frac{\mathrm{d}U_f}{\mathrm{d}t} = \sqrt{\frac{t_e^*}{t^* - t}}, \tag{31}$$

$$\frac{(\overline{u}_{uf}^* - \overline{u}_{uf})}{\overline{u}_{uf}^*} = \sqrt{\frac{t^* - t}{t_e^*}}, \qquad \frac{t_e^*}{\overline{u}_{uf}^*}\frac{\mathrm{d}\overline{u}_{uf}}{\mathrm{d}t} = \sqrt{\frac{t_e^*}{t^* - t}}, \tag{32}$$

showing the runaway of the acceleration of the flame front $\mathrm{d}U_f/\mathrm{d}t$ and of the gas-flow $\mathrm{d}\overline{u}_{uf}/\mathrm{d}t$ when the critical condition is approached. Notice that the runaway is always produced regardless of the elongation rate $\sigma^{-1}(\mathrm{d}\sigma/\mathrm{d}t)|_{\sigma=\sigma^*}$, the square-root scaling law taking a universal form (free from parameters) when using the reduced time $\tau \equiv t/t_e^*$. The acceleration of the laminar flame-speed $\mathrm{d}U_L/\mathrm{d}t$ and/or $\mathrm{d}U_b/\mathrm{d}t$ also diverges according to the same scaling laws as (31)-(32), the critical values U_L^* and U_b^* being markedly subsonic.

6. Beyond self-similarity. Formation of a shock on the flame front

The self-similar solutions are accurate as long as the compressible waves are sufficiently fast to make the flow quasi-uniform and quasi-steady. More precisely, the transit time of acoustic waves in both directions between the flame and the lead shock should be shorter than the time scale of the modifications of the flame speed. This approximation is no longer valid for large accelerations of the flame all the more so as the lead shock is far away from the flame, and more particularly near the turning point where the acceleration diverges pointing out the strong limitation of the self-similar solutions.

The two-dimensional numerical simulations of Liberman and coworkers [7, 9] show a suc-

cession of compression waves steepening into shocks ahead of the flame in close proximity of its front. A shock seems to sit at the tip of the elongated flame just before DDT. The flame propagating with a subsonic speed (relative to the upstream gas) while the shock is supersonic, a shock is more likely formed spontaneously inside the inner flame structure producing quasi-instantaneously the blow-up of the flame structure before escaping downstream into the unreacted gas. Understanding of the abrupt DDT of a self-accelerating flame near the turning point requires the full solution of the unsteady problem, including the inner structure of the laminar flame. Unfortunately unsteadiness of the inner structure can be solved analytically only for much milder situations [24]. The study should be performed numerically in a one-dimensional geometry within the framework of the piston model using a high-order spectral difference flow solver. This will be presented in forthcoming papers. We limit our attention below to the simple waves that are generated in the unreacted gas by the large acceleration of a piston approaching the critical velocity of the turning point. The objective is to show that the unsteady compressible waves lead to the formation of a singularity of the flow on the piston when the piston velocity reaches the critical velocity.

6.1. Theoretical analysis

Using the characteristics method of Riemann [25], an analytical solution of the isentropic Euler equations can be obtained for the simple waves issued from a piston starting to move in an inert gas initially at rest. Following the presentation in [26], the flow $u(x,t)$ of a simple compression wave propagating from left to right in a perfect gas, written in a Galilean frame where $\lim_{x\to\infty} u = 0$, is solution of the equation

$$x = \left[\frac{(\gamma+1)}{2}u + a_\infty\right] t + F(u) \tag{33}$$

where a_∞ is the initial sound speed of the gas at rest and $F(u)$ is a function of the flow velocity given by the condition at the piston $x = X_p(t)$: $u(X_p(t),t) = \mathrm{U}_p(t) = \mathrm{d}X_p/\mathrm{d}t$. Limited to isentropic conditions, this solution is no longer valid after the apparition of a singularity in the flow gradient. The known function $X_p(t)$ increasing monotonously with the time, the function $F(u)$ is obtained from (33) applied at the boundary condition $x = X_p(t) : u = \mathrm{U}_p(t)$, using the functions $X_p(\mathrm{U}_p)$

and $t(\mathrm{U}_p)$ obtained by inversion of $\mathrm{U}_p(t)$. For the classical problem corresponding to a power law $X_p(t) \propto t^{n+1}$ with $n > 1$ for $t \geqslant 0$ and $\mathrm{d}X_p/\mathrm{d}t = 0$ for $t < 0$, the initial acceleration is zero $\mathrm{d}^2X_p/\mathrm{d}t^2|_{t=0^+} = 0$. The analytical solution presented in [26] then shows that the flow gradient $\partial u/\partial x$ diverges at a finite distance ahead of the piston after a finite time, yielding the place and time of formation of the shock wave. This is no longer the case for $n < 1$; the singularity of the initial acceleration of the piston velocity $\mathrm{d}^2X_p/\mathrm{d}t^2|_{t=0^+} = \infty$ causes the shock to be formed instantaneously on the piston. None of these cases correspond to an accelerating flame approaching the critical velocity of a turning point. However, the divergence of the acceleration suggests that a shock will be formed on the piston when the piston velocity reaches the critical value. The corresponding analytical study is presented now.

Consider a piston propagating in an inert gas with a velocity $\mathrm{U}_P(t)$ following the scaling law (31) written, using the non-dimensional time $\tau = t/t_e^*$, $\tau^* \equiv t^*/t_e^*$, in the form

$$0 < \tau \leqslant \tau^* : \quad \frac{\mathrm{U}_P^* - \mathrm{U}_P}{\mathrm{U}_P^*} = \sqrt{(\tau^* - \tau)}, \quad \frac{1}{\mathrm{U}_P^*}\frac{\mathrm{d}\mathrm{U}_P}{\mathrm{d}\tau} = \frac{1}{2}\frac{1}{\sqrt{\tau^* - \tau}}, \tag{34}$$

with typically $\mathrm{U}_P^* = 1.2\, a_\infty$ as in the flame problem considered in § 4. In order to stress the effect of the divergence of the acceleration at the turning point, consider the scaling law (34) for $\tau \geqslant 0$, the velocity of the piston being constant for $\tau \leqslant 0 : \mathrm{U}_P(\tau) = \mathrm{U}_P(0)$ and the flow constant and uniform; $\tau \leqslant 0 : u(x,\tau) = \mathrm{U}_P(0)$ and $a(x,\tau) = a_\infty \ \forall x > X_P(t)$. In other words we consider that unsteadiness is negligible for $\tau \leqslant 0$ so that the self-similar solution is valid initially with a shock wave at infinity. The piston starting to accelerate at $\tau = 0^+$, the boundary condition of the flow at infinity is $\lim_{x\to\infty} a(x,\tau) = a_\infty$ and $\lim_{x\to\infty} u(x,\tau) = \mathrm{U}_P(0)\ \forall\tau$. According to (34)

$$\tau \leqslant 0 : \qquad \mathrm{U}_P(\tau) = \mathrm{U}_P(0) \quad \Rightarrow \quad \frac{\mathrm{U}_P^* - \mathrm{U}_P(0)}{\mathrm{U}_P^*} = \sqrt{\tau^*} \tag{35}$$

so that, in the Galilean frame moving with the initial flow, equation (34) takes the form

$$0 < \tau \leqslant \tau^* : \quad 0 \leqslant \frac{\mathrm{U}_P(\tau) - \mathrm{U}_P(0)}{\mathrm{U}_P^*} = \sqrt{\tau^*} - \sqrt{(\tau^* - \tau)}. \tag{36}$$

For γ fixed, there are only two free non-dimensional parameters in this problem

$$\tau^* \equiv t^*/t_e^* \qquad \text{and} \qquad m^* \equiv \mathrm{U}_P^*/a_\infty. \tag{37}$$

The only length scale in the problem being $l \equiv a_\infty t_e^*$, one introduces the non-dimensional coordinate ξ and the non-dimensional position of the piston $\xi_P(\tau)$

$$\xi \equiv x/(a_\infty\, t_e^*), \qquad \xi_P(\tau) = X_P(t)/(a_\infty\, t_e^*) \tag{38}$$

where $\mathrm{d}X_P/\mathrm{d}t = \mathrm{U}_P(t)$ and $X_P(0) = 0$, the origin of the x-axis being the initial position of the piston. The trajectory of the piston, obtained by integrating the first equation in (34), takes the non dimensional form

$$0 < \tau \leqslant \tau^* : \quad \xi_P(\tau) = \left[\tau\,\sqrt{\tau^*} + \frac{2}{3}(\tau^* - \tau)^{3/2} - \frac{2}{3}\tau^{*3/2}\right] m^*, \qquad \xi_P^* \equiv \frac{X_P^*}{a_\infty\, t_e^*} = \frac{1}{3}\tau^{*3/2} m^* \tag{39}$$

$$\xi_P(\tau) - \xi_P^* = \left[-(\tau^* - \tau)\,\sqrt{\tau^*} + \frac{2}{3}(\tau^* - \tau)^{3/2}\right] \tag{40}$$

$X_P^* \equiv X_P(t^*)$ being the distance separating the final position of the piston at $t = t^*$ from its initial position ($t = 0$). Introducing the notations

$$\dot{\xi}_P(\tau) \equiv \mathrm{d}\xi_P/\mathrm{d}\tau = [\mathrm{U}_P(t) - \mathrm{U}_P(0)]/a_\infty, \qquad \ddot{\xi}_P(\tau) \equiv \mathrm{d}^2\xi_P/\mathrm{d}\tau^2 = t_e^*[\mathrm{d}\mathrm{U}_P(t)/\mathrm{d}t]/a_\infty \tag{41}$$

for the reduced velocity and acceleration of the piston in the Galilean frame, (36)-(40) read

$$0 < \tau \leqslant \tau^* \;:\; \dot{\xi}_P(\tau) = \left[\,\sqrt{\tau}^* - (\tau^* - \tau)^{1/2}\right] m^*, \qquad \ddot{\xi}_P(\tau) = \frac{m^*}{2(\tau^* - \tau)^{1/2}}, \tag{42}$$

$$\tau = \tau^* \;:\; \xi_P(\tau^*) = \frac{1}{3}\tau^{*3/2} m^*, \quad \dot{\xi}_P(\tau^*) = m^*\,\sqrt{\tau^*}, \quad \lim_{\tau\to\tau^*} \ddot{\xi}_P(\tau) = \frac{m^*}{2(\tau^* - \tau)^{1/2}}, \tag{43}$$

$$\tau = 0^+ \;:\; \xi_P(0) = 0, \qquad \dot{\xi}_P(0) = 0, \qquad \ddot{\xi}_P(0^+) = \frac{m^*}{2\,\tau^{*1/2}}. \tag{44}$$

$$\tau^* \leqslant 0 \;:\; \xi_P(0) = 0, \qquad \dot{\xi}_P(\tau) = 0, \qquad \ddot{\xi}_P(\tau) = 0. \tag{45}$$

For a situation similar to the flame in § 4, the piston is subsonic at the initial condition $\mathrm{U}_P(0)/a_\infty <$

1 and supersonic at criticality $\mathrm{U}_P(t^*)/a_\infty = m^* > 1$. Introducing the non-dimensional flow velocity $v(\xi,\tau)$ in the Galilean frame moving with U(0),

$$v(\xi,\tau) \equiv [u - \mathrm{U}_P(0)]/a_\infty, \quad \xi \equiv x/(a_\infty t_e^*); \qquad \tau \leqslant 0 : \ v = 0, \tag{46}$$

the boundary conditions at the piston and at infinity yield

$$0 < \tau \leqslant \tau^* \ : \quad v_P(\tau) \equiv v(\,\xi_P(\tau)\,,\tau) = \dot\xi_P(\tau) - \dot\xi_P(0) = \left[\tau^{*1/2} - (\tau^* - \tau)^{1/2}\right] m^* \tag{47}$$

$$\tau = \tau^* \ : \quad v_P^* \equiv v(\,\xi_P(\tau^*),\,\tau^*) = \tau^{*1/2} m^*; \qquad \xi \to \infty : \ a = a_\infty,\ v(\xi,\tau) = 0 \ \ \forall\tau. \tag{48}$$

In this frame, the piston is initially at rest, its velocity $\dot\xi_P(\tau)$ in (41) is nil at $\tau = 0$, $\dot\xi_P(0) = 0$ and, according to (43), becomes supersonic at $\tau = \tau^*$ if $1/m^* < \tau^{*1/2} \Rightarrow \dot\xi_P(\tau^*) > 1$, $[\mathrm{U}_P^* - \mathrm{U}_P(0)]/a_\infty > 1$.

Formation of a shock in a finite time $\tau = \tau_s$ is produced by the acceleration of the piston which presents a jump $m^*/(2\sqrt{\tau^*})$ at the initial condition, see (44)-(45). An analytical expression of τ_s can be obtained following the method in [26]. Introducing the constant term ξ_P^* and the function $f(v) \equiv F(u)/a_\infty t_e^* - \xi_P^*$ the reduced form of (33) in which $u \to u - \mathrm{U}_P(0)$ takes the form

$$\xi - \xi_P^* = \left[\left(\frac{\gamma+1}{2}\right)(v_P^* - v) - \left(\frac{\gamma+1}{2}\right)v_P^* - 1\right]\left[(\tau^* - \tau) - \tau^*\right] + f(v). \tag{49}$$

The function $f(v_P)$ is computed by the boundary condition at the piston $\xi = \xi_P(\tau)$: $v = v_P(\tau)$ after eliminating τ in favor of $v_P(\tau)$ by using (47)-(48) $(\tau^* - \tau) = (v_P^* - v_P)^2/m^{*2}$ and (40) in the form

$$\xi_P - \xi_P^* \ = \ \left[-\frac{(v_P^* - v_P)^2}{m^{*2}}\sqrt{\tau^*} + \frac{2}{3}\frac{(v_P^* - v_P)^3}{m^{*3}}\right] m^*. \tag{50}$$

Introducing the expressions $(\tau^* - \tau) = (v_P^* - v_P)^2/m^{*2}$ and (50) respectively into the right-hand side and the left-hand side of (49) yields the expression of $f(v_P)$, namely the function $f(v)$ in the form

$$f(v) = \left(\frac{2}{3} - \frac{\gamma+1}{2}\right)\frac{(v_P^* - v)^3}{m^{*2}} + \left(\frac{\gamma+1}{2}v_P^* + 1 - m^*\sqrt{\tau^*}\right)\frac{(v_P^* - v)^2}{m^{*2}} - \frac{\gamma+1}{2}\tau^* v - \tau^*. \tag{51}$$

The relation $f(0) = -m^*\tau^{*3/2} = -\xi_P^*$ which is obtained from (51) by using (48) $v_P^* = \tau^{*1/2} m^*$,

confirms that, according to (49), the trajectory in the medium at rest of the leading edge of the compression wave ($v = 0$) is effectively $\xi = \tau$+constant, corresponding to a propagation velocity equal to the sound speed a_∞, as it should be for a weak discontinuity. Using the notation $f'(v) \equiv \mathrm{d}f/\mathrm{d}v$, the derivative of (51) with respect to v yields

$$f'(v) = -3\left(\frac{2}{3} - \frac{\gamma+1}{2}\right)\frac{(v_P^* - v)^2}{m^{*2}} - 2\left(\frac{\gamma+1}{2}v_P^* + 1 - m^*\sqrt{\tau^*}\right)\frac{(v_P^* - v)}{m^{*2}} - \frac{\gamma+1}{2}\tau^*, \tag{52}$$

while the partial derivative of (49) with respect to ξ

$$1 = \left[\frac{\gamma+1}{2}t + f'(v)\right]\frac{\partial v}{\partial \xi} \tag{53}$$

shows that the time $\tau = \tau_s$ and the velocity $v = v_s$ at which the flow gradient diverges $|\partial v/\partial \xi| = \infty$, are linked by the relation

$$\tau_s = -\frac{2}{\gamma+1}f'(v_s). \tag{54}$$

According to (52), equation (54) is verified for $\tau_s = \tau^*$, $v = v^*$ and, according to (33) and (49), the place of formation of the singularity is the critical position of the piston $\xi_s = \xi_P^*$. This shows that a singularity of the flow is systematically formed on the piston at the critical time $\tau = \tau^*$.

However equation (49) is limited to isentropic flows and one has to check wether or not another singularity can be formed before τ^*. It turns out that this is possible at the leading edge of the compression wave, $v = 0$. Introducing $\xi_P^* = m^*\tau^{*3/2}$ and $v = 0$ in (52) leads to $f'(0) = -2\sqrt{\tau^*}/m^*$. Therefore, according to (54), a singularity can be formed ahead the piston at time

$$\tau_s = \frac{4}{\gamma+1}\frac{\sqrt{\tau^*}}{m^*}, \tag{55}$$

which is earlier than τ^* if

$$\frac{4}{\gamma+1}\frac{1}{m^*} < \sqrt{\tau^*}. \tag{56}$$

The relation $t^*/t_e^* > [4/(\gamma+1)]^2 a_\infty/\mathrm{U}_P^*$ in (56) corresponds to a time t^* sufficiently long for reaching the critical velocity after the piston started to accelerate. This also corresponds to a sufficiently long distance separating the initial and final positions of the piston $X_P^*/(a_\infty t^*) > 4/(\gamma+1)$. No other singularity can be formed for $0 \leqslant \tau < \tau^*$ since no inflection point of the flow field can be produced in the rarefaction wave $\mathrm{d}^2 f/\mathrm{d}\xi^2 = 0$ simultaneously with $|\mathrm{d}f/\mathrm{d}\xi| = \infty$. Therefore, the relation (56) corresponds to a first singularity formed ahead of the piston. The opposite condition

$$\sqrt{\tau^*} < \frac{4}{\gamma+1}\,\frac{1}{m^*} \tag{57}$$

corresponds to a first singularity formed on the piston. Notice the difference between the two singularities, the latter being formed at the maximum flow velocity in the compression wave $u = \mathrm{U}_P^*$ while the former is formed at the minimum $u = \mathrm{U}_P(0)$ ($\nu = 0$).

6.2. Numerical simulation

All these analytical results have been verified by the direct numerical simulation of the solutions of the Euler equations by using the high-order spectral difference solver developed by Lodato [21]. The details of the implementation of the numerical scheme may be found in [21] and are not reproduced here, only the most important features of the numerics and their validation is given in a footnote [1]. The one-dimensional non-steady flow of a perfect gas which is generated by an adiabatic piston has been solved numerically here when the piston velocity satisfies the power law (34)-(35). Before the first formation of a finite-time singularity ($t = t_s$), the analytical expression of

[1] The Euler equations are solved in their fully compressible form using the spectral-difference method [27, 28]. Each one-dimensional cell constitutes an element in which the coordinates are normalized. The solved signal is reconstructed within this finite volume element from n solution points with a degree $n-1$ polynomial. Similarly, degree n polynomials are used to reconstruct the fluxes of the transported variables from $n+1$ flux points. The Gauss-Legendre quadrature points are retained for locating the solution points, whereas the flux points are selected to be the Gauss-Legendre quadrature points of order $n-1$ plus the two ends points. This approach can be proved to be linearly stable whatever the order of accuracy (i.e., the value of n), to be optimal for the reduction of aliasing errors and, finally, to provide good conditioning [27, 28].The reconstructed fluxes are only element-wise continuous, and discontinuous across the cell interfaces. A Riemann solver is employed to compute a common flux at cell interfaces. Here, the Roe solver with entropy fix is used [29, 30]. The choc capturing technique is based on the analysis of the linear decay of the modes of the interpolated solution, with a calibration made from manufactured solutions [31]. Numerous validations of this numerical framework for the simulations of shock waves may be found in [31–33].

the flow obtained from (33) is verified with an excellent accuracy[2]. This is also true for the condition (55) separating the case of a first finite-time singularity at the leading edge of the compression wave ($t = t_s$, $u = 0$) from the case of a first singularity on the piston, $x = X_P(t_s)$, $u = U_P(t_s)$. Moreover, when, in agreement of (56), the first singularity is formed ahead of the piston at the leading edge of the compression wave, the numerical simulation shows that a second singularity of the flow gradient is systematically formed on the piston at the critical condition $t_s = t^*$. This result cannot be obtained rigorously by the analytical approach since equation (33) is limited to an isentropic condition so that the theoretical analysis is no longer valid after the formation of a first shock. If the piston velocity is kept fixed after the critical condition ($t > t^* : U_P = U_P^*$), the supersonic velocity of the singularity formed on the piston being larger than U_P^*, this singularity leaves the piston to form a final shock ahead of the piston, leading to the self-similar solution after a time proportional to t_e^*. An example of such a numerical simulation is given in figure 4.

6.3. Discussion

These theoretical and numerical results suggest that a shock can be formed inside the inner flame structure on the tip of a self-accelerating elongated flame-front as soon as its velocity reaches the critical value of the turning point of the self-similar solutions[3]. However, for an abrupt DDT at the critical velocity of the self-similar solutions, the increase of temperature should be sufficiently strong to blow up the inner flame structure quasi-instantaneously before the shock escapes the inner structure of the subsonic flame. This looks possible for gaseous mixtures that are sufficiently energetic even though the flow inside the inner flame structure which is increasing in the propagation direction (from the burnt to the unburnt gas side) is not in favor of shock formation, see figure 3. Therefore, the singularity is expected to be formed at a point inside the premixed zone near the cold side where the initial gradient of the flow is not large but the temperature sufficiently large for producing fast self-ignition, which was not possible outside the flame structure where the temperature of the unreacted gas is too low. Moreover figure 4 suggests that a train of successive

[2]The numerical code has been also successfully tested on the piston problem $t \geqslant 0$: $X_p(t) \propto t^{n+1}$ with $n > 0$ and $\mathrm{d}X_p/\mathrm{d}t = 0$ for $t < 0$ for which an analytical solution has long been known [26].

[3]It could seem questionable to work beyond self-similarity near the critical condition using the scaling laws of the self-similar solutions. This is not so because the feedback of the self-similar solution on the flame, namely the increase of the gas temperature, is similar to that of a compression wave.

shock waves can be produced if the time t_e^* is sufficiently short. These fundamental aspects of the DDT problem will be investigated numerically in forthcoming papers with the one-dimensional piston-model using appropriate (high-quality) numerics [21]. Since shocks cannot be formed in the stretched multidimensional flow of burned gas inside the elongated front, the adiabatic piston is applied at the exit of the reaction zone with the velocity in (5) $u_{bf} = [\sigma(t) - 1](\rho_{uf}/\rho_{bf})U_L$, see figure 3 in the legend of which the formulation of the unsteady problem is briefly formulated for a reacting flow.

7. Conclusion and perspectives

Comparison of the 2010 experiments [6, 7] with the theoretical results obtained with the one-dimensional piston-model for very energetic mixtures, shows that the sudden DDT at the tip of a self-accelerating elongated flame occurs when the flame velocity reaches the critical value at the turning point of the self-similar solutions. This suggests that the feedback mechanism based on the back-flow is involved in these experiments. The role of the back-flow of burnt gas towards the flame tip is all the more important since the density ratio across the laminar flame is large and the thermal sensitivity of the laminar flame speed weak.

Moreover, the solutions of the upstream-running simple waves that are generated in an inert gas from an accelerating piston have shown that, due to the singularity of the acceleration at the turning point, a shock is formed on the piston when the critical velocity is reached. This suggests the formation of a finite-time singularity inside the inner structure of the flame, in agreement with the multi-dimensional numerical simulations [7, 9] performed by Liberman and co-authors in the experimental conditions. A detailed analysis of the sudden transition is left for future one-dimensional numerical simulations of DDT using the piston-model.

The small elongation of the finger flame at the critical condition, of the order of the tube diameter in § 4, suggests that cellular flames of very energetic mixtures could also experience DDT in free space through the mechanism described in the present paper. Typical examples are the Rayleigh-Taylor unstable flames sustained by nuclear reactions [3] explaining DDT in type I supernovae which was recently revisited [34].

Acknowledgments

The authors are grateful to Forman Williams for enlightening discussions and to Guido Lodato for setting up the numerical test case in his high-order Spectral Difference flow solver. The authors are also grateful to Grisha Sivashinsky and Michael Liberman for insightful comments. This work is supported by ANR (Agence Nationale de la Recherche) under the project 18-CE05-0030 'ReDDT' (Revisiting Deflagration to Detonation Transition in the context of carbon-free energy production).

References

[1] J.M. Meyer, P.A Urtiew, A.K. Oppenheim, On the inadequacy of gas dynamic processes for triggering the transition to detonation, Combust. Flame, 14-1 (1970) 13–20.

[2] J.H.S. Lee, The detonation phenomenon, Cambridge University Press, 2008.

[3] P. Clavin, G. Searby, Combustion Waves and Fronts in Flows, Cambridge University Press, 2016.

[4] K.I. Shchelkin, Ya.K. Troshin, Gasdynamics of Combustion, Mono Book Corp., 1965.

[5] M. Wu, M.P. Burke, S.F.Son, R.A. Yetter Flame acceleration and the transition to detonation of stoichiometric ethylee/oxygen in microscale tubes, Proc. Comb. Inst., 31 (2007) 2429–2436.

[6] M. Kuznetsov M. Liberman, I. Matsukov Experimental study of the preheated zone formation and deflagration to detonation transition, Combust. Sci. and Tech., 182 (2010) 1628–1644.

[7] M.A. Liberman, M.F. Ivanov, A.D. Kiverin, M.S.Kuznetsov, A.A Chukalovsky, T.V. Rakhimova, Deflagration-to-detonation transition in high reactive combustible mixtures, Acta. Astronautica, 67 (2010) 688–701.

[8] M. Wu, C. Wang Reaction propagation modes in millimeter-scale tubes for ethylene/oxygen mixtures, Proc. Comb. Inst., 33 (2011) 2287–2293.

[9] M.F. Ivanov, A.D. Kiverin, M.A. Liberman, Hydrogen-oxygen flame acceleration and transition to detonation in a a detailed chemical reaction model, Phys. Rev. E, 83 (2011) O56313.

[10] Ya.B. Zeldovich, Regime classification of an exothermic reaction with nonuniform initial conditions, Combust. Flame 39 (1980) 211–214.

[11] R.W. Houim, A. Ozgen, E.S. Oran, The role of spontaneous waves in the deflagration-to-detonation transition is submillimetre channels, Combust. Theory Model., 20(6) (2016) 1068–1087.

[12] W. Han, Y. Gao, C.K.Law, Flame acceleration and deflagration-to-detonation transition in micro- and macro-channels: An integrated mechanism study , Combust. Flame 176 (2017) 285–298.

[13] B. Deshaies, G. Joulin, Flame-speed sensitivity to temperature changes and the Deflagration-to-Detonation Transition, Combust. Flame 77 (1989) 202–212.

[14] L. Kagan, G. Sivashinsky, Parametric transition from deflagration to detonation: Runaway of fast flames, Proc. Combust. Inst., 36 (2017) 2709–2715.

[15] A. Koksharov, V. Bykov, L. Kagan, G. Sivashinsky, Deflagration-to-detonation transition in an unconfined space, Combust. Flame, 195 (2018) 163–169.

[16] P.V. Gordon, L. Kagan, G. Sivashinsky, Parametric transition from deflagration to detonation revisited: Planar Geometry, Combust. Flame, 211 (2020) 465–476.

[17] V.N. Gamezo, A.Y. Poludnenko, E.S. Oran, One-dimensional evolution of fast flame, Proceedings of 23rd ICDERS, Irvin, USA, 2011, July 24-29.

[18] B. Ponizy, A. Claverie, B. Veyssière, Tulip flame - the mechanism of flame front inversion, Combust. Flame, 161 (2014) 3051–3062.

[19] V. Bychkov, A.Petchenko, V. Akkerman, L.E Erikson, Theory and modeling of accelerating flames in tubes, Phys. Rev. E 72 (2005) 046307.

[20] D.M. Valiev, V. Bychkov, V. Akkerman, L.E Erikson, Different stages of flame acceleration from slow burning to Chapman-Jouguet deflagration , Phys. Rev. E 80 (2009) 036317.

[21] G. Laudato, Characteristic modal shock detection for discontinuous methods, Comput. Fluids. 179 (2019) 309–333.

[22] C. Clanet, G. Searby, On the tulip flame phenomenon, Combust. Flame 105 (1996) 225–238.

[23] Ya.B. Zeldovich, D.A Frank-Kamenetskii, A theory of thermal flame propagation, Acta Phys. Chim. 9 (1938) 341–350.

[24] P. Clavin, P. Pelce, L. He, One-dimensional vibratory instability of planar flames propagating in tubes, J. Fluid Mech. 216 (1990) 299–322.

[25] B. Courant, K.O Friedrichs, Supersonic flow and shock waves, Interscience Publishers, John Wiley and Sons, 1948.

[26] L. Landau, E.M Lifshitz, Fluid Mechanics, Pergamon Press, 1959.

[27] A. Jameson, A proof of the stability of the spectral difference method for all orders accuracy, J. Sci. Comput., 45-1 (2010) 348–358.

[28] A. Jameson, P.E. Vincent, P.Castonguay, On the non-linear stability of flux reconstruction schemes, J. Sci. Comput., 50-2 (2012) 434–445.

[29] P.L. Roe, Approximate Riemann solvers, parameter vector and difference schemes, Journal of Computational Physics, 43 (1981) 357–372.

[30] A. Harten, High resolution schemes for hyperbolic conservation laws, Journal of Computational Physics, 49 - 3 (1983) 357–393.

[31] G. Lodato, L. Vervisch, P. Clavin, Direct numerical simulation of shock wavy-wall interaction: analysis of cellular shock structures and flow patterns, J. Fluid Mech., 789 (2016) 221–258.

[32] B. Denet, L. Biamino, G. Lodato, L. Vervisch, P. Clavin, Model equation for the dynamics of wrinkled shock waves. Comparison with DNS and experiments, Combust. Sci. and Tech., 187 (2015) 296–323.

[33] G. Lodato, L. Vervisch, P. Clavin, Numerical study of smoothly perturbed shocks in the Newtonian limit, Flow Turbulence and Combustion, 99-3 (2017) 887–908.

[34] P.V. Gordon, L. Kagan, G. Sivashinsky, Parametric transition from deflagration to detonation in stellar medium, Phys. Rev. E, 103 (2021) 033106-1-9.

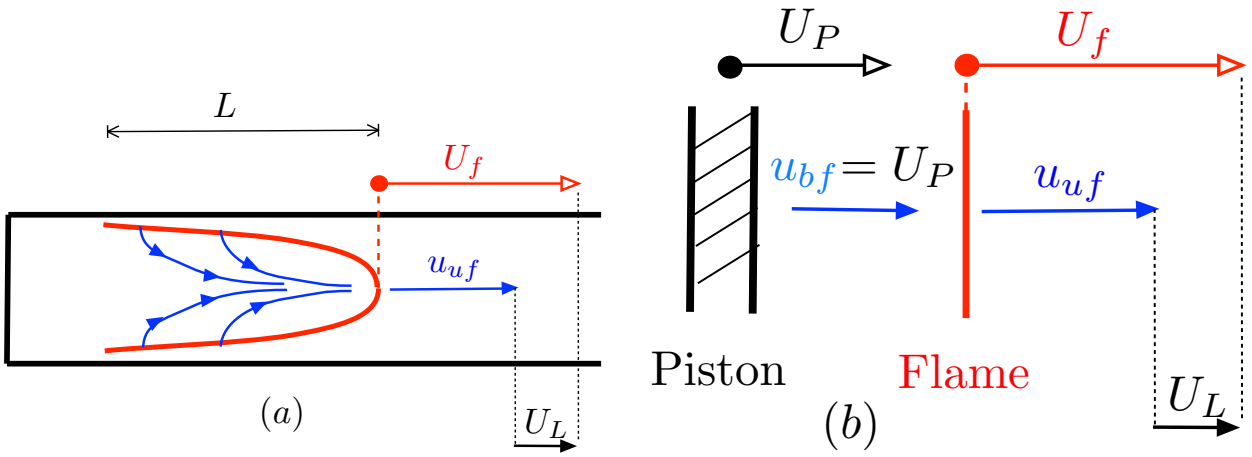

Figure 1: (a): Sketch of the self-accelerating elongated flame propagating in the laminar regime. The streamlines of the burnt-gas flow issuing from the lateral wings of the flame front and oriented towards the flame tip are shown in blue. (b): One-dimensional piston model. The velocity of the piston $U_p(t)$ increases with the extension of the flame front $L(t)$ and also with the temperature of the burnt gas (through the laminar burning velocity measured in the burnt gas), see (1). This model defines the simplest configuration of the double mechanisms leading to DDT at the tip of an elongated flame : firstly the compressional heating by the upstream-running simple waves generated in the unburned gas by the flame acceleration, $dU_f/dt > 0$, and secondly the convective motion of the flame (at the tip) caused by the back-flow of burnt-gas, $u_{bf} \gg U_L$ for very energetic mixtures $\rho_u \gg \rho_b$, $U_b \gg U_L$.

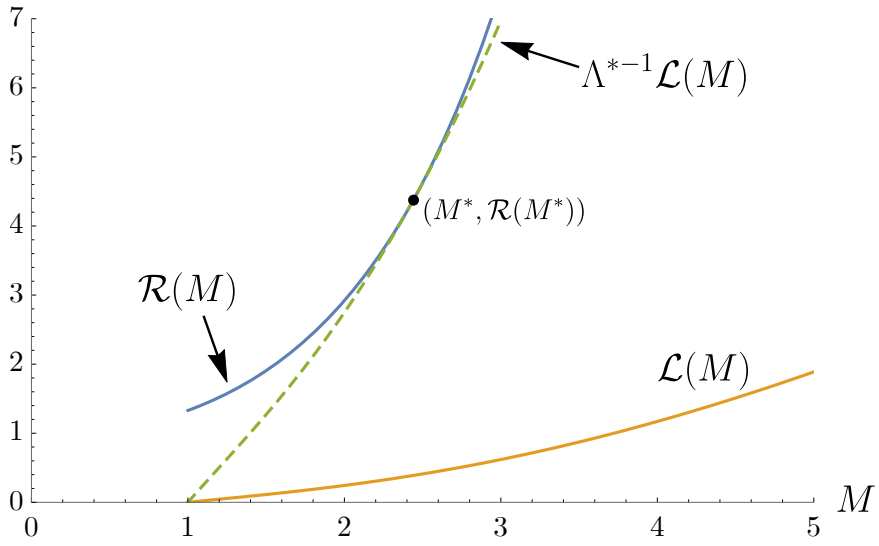

Figure 2: Plots of $\mathcal{L}(M)$ in (26) and $\mathcal{R}(M)$ in (27) for $\gamma = 1.4$, $q = 9$ and $\beta_o = 1.25$. The tangency of the graphs $\Lambda^{-1}\mathcal{L}(M)$ and $\mathcal{R}(M)$ is obtained for $\Lambda^* = 0.089$ at $M^* = 2.44$.

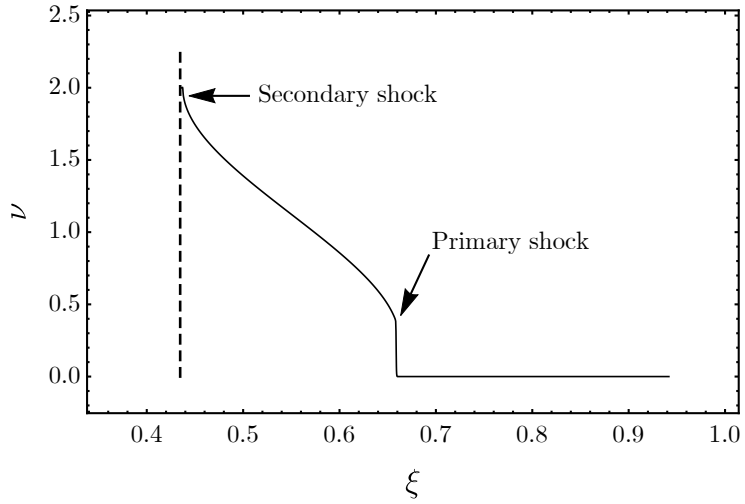

(a) $\tau = \tau^* = 0.64$

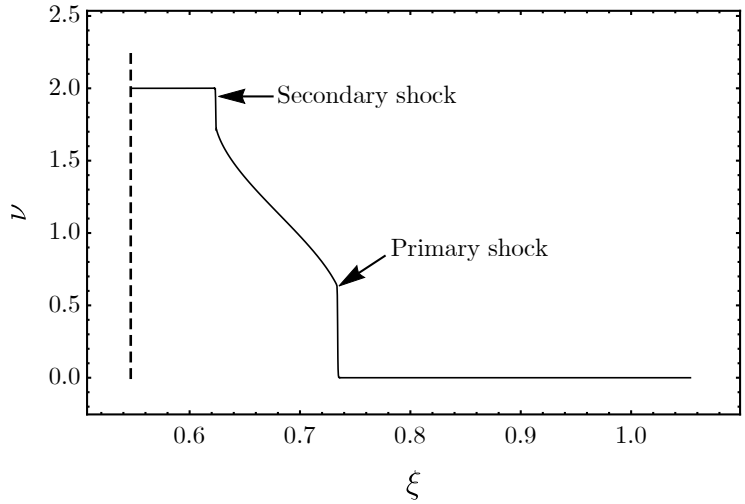

(b) $\tau = 0.7 > \tau^*$

Figure 3: Velocity profiles for the problem of shock formation by an accelerating piston (34), as obtained in the case (56) by a numerical simulation, with $m^* = 2.5$ and $\tau^* = 0.64$, $\sqrt{\tau^*} = 0.8 > (1/m^*)4/(\gamma + 1) = 0.666$. The dashed line represents the position of the piston, which is moving from left to right. (a) At $\tau = \tau^*$, the primary shock formed earlier at the tip of the compression wave can be observed, as well as the secondary shock forming on the piston. (b) In this figure, the piston continues to move with a constant velocity U_P^* after τ^*, while the secondary shock is catching up with the primary one. The increase of the gas temperature at the piston is similar to that in the self-similar solution with the piston velocity U_P^*.

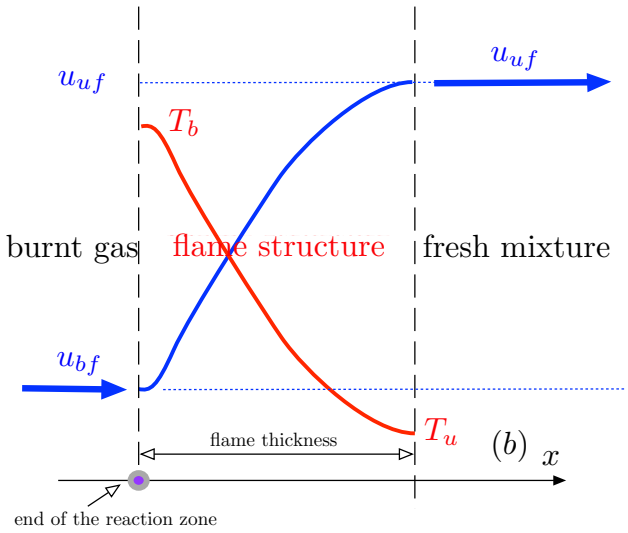

Figure 4: The compressible version of the reactive Navier-Stokes equations have to be solved in a one-dimensional geometry using appropriate (high-quality) numerics [21]. A quasi-isobaric flame is ignited on the closed end of a tube, the other end being open. After a while (transit time across the laminar flame) the flame reaches a quasi-steady state. An adiabatic piston is then applied at the exit of the reaction zone with a velocity $u_{bf} = [\sigma(\tau) - 1](\rho_{uf}/\rho_{bf})U_L$ for a given function $\sigma(t)$ with $\sigma(0) = 1$. In this expression, the laminar flame speed $U_L(T_{uf}, \rho_{uf})$ and the density ratio correspond to $T_{uf}(t)$ and $\rho_{uf}(t)$ obtained by the simulation with an eventual time delay to take into account the transit time of the acoustical waves across the burned gas enclosed in the elongated flame. Other expressions of the back-flow $u_{bf}(t)$ can be used, for example the one obtained from $\sigma(t)$ and $u_{uf}(t)$ by a spatial integration of the instantaneous distribution of the rate of heat release.